Impact of surface orientation of structures on their seasonal deformation: a case study in the UK

Ali ALGADHI[1,*], **Panos PSIMOULIS**[2,3], **Athina GRIZI**[4], and **Luis NEVES**[3]

[1] *Dept. of Civil Engineering, King Saud University, Riyadh, Saudi Arabia, (aalgadhi@ksu.edu.sa)*

[2]*Nottingham Geospatial Institute, University of Nottingham, Nottingham, UK, (Panagiotis.Psimoulis@nottingham.ac.uk)*

[3]*Dept. of Civil Engineering, University of Nottingham, Nottingham, UK, (Luis.Neves@nottingham.ac.uk)*

[4]*Region of Western Greece, Patras, Greece, (a.grizi@pde.gov.gr)*

[*]*corresponding author*

Abstract

Solar radiation varies in magnitude and duration throughout the year causing changes in solar absorption of structures, leading to seasonal movement; expansion during the hot season and contracting during the cold season. This seasonal movement can be dangerous for the health of structures if they exceed some limits. This paper aims to investigate the effect of the surface orientation of structures on the amplitude of deformation caused by the solar radiation through measurements using Terrestrial Laser Scanner (TLS). The monitored structure involves sheet piles, a capping beam, and a brick wall. The sheet piles consist of flanges and webs that have various surface orientation, and consequently this paper monitors the seasonal deformation of different parts of the sheet piles using one of the main cloud-comparison techniques; the Multiscale-Model-to-Model-Cloud-Comparison (M3C2) method. The structure was scanned five times starting from November 2020 with two scans each year: one in June and the other in November. The results show a clear difference between the different parts of the sheet piles; about $\pm 25\%$ of rise/decline in the seasonal lateral movement (± 1 *mm* of change with respect to 4 *mm* of lateral movement in the capping beam) that is caused by the change in surface orientation. This suggests that the seasonal deformation of structures can be slightly controlled by the surface orientation. This is significant especially considering the climate change and its implications on the variation of solar absorption of structures.

Keywords: Climate change, seasonal movement, SHM, sheet piles, TLS, LiDAR, M3C2

Received: 9th December 2024. Revised: 28th February 2025. Accepted: 13th March 2025.

1 Introduction

Seasonal deformation in structures is one of the common types of semi-static deformations, which is a deformation that occur over a long period of time (e.g., few months) but is not permanent. The thermal variation between the seasons is a main cause of this type of deformation in structures (Breña et al., 2007; Westgate et al., 2015). Some studies also suggest that the impact of solar radiation increases as the normal direction of the surface is aligned with the sunlight direction. Kromanis and Kripakaran (2016) seem to support that in their experiment by concluding that the parts of the monitored structure that was closer to the source of heat had larger thermal deformation. Furthermore, the surface orientation with respect to the sun was found a main factor in the absorbed solar radiation for the solar panels orientation (Chwieduk and Bogdanska, 2004; Jafarkazemi and Saadabadi, 2013). Therefore, the thermal deformation might be larger for the structures that are oriented directly towards the sun most of the daytime.

The seasonal deformation is expected to be a critical issue in terms of deformations of structures as the climate change affects the variation in temperature and solar radiation between seasons (Apriyono et al., 2022). The impact of climate change also varies spatially leading to larger impact on some areas (Portmann et al., 2009). Therefore, these deformations should be monitored to ensure the health state of structures.

To detect these small seasonal deformations (usually the deformation is within few millimetres), many techniques has been adopted but the contactless techniques and especially the LiDAR sensors have been of great interest recently due to their rapid and accurate measurements (Algadhi et al., 2025). The point clouds from different epochs can be compared and the distance between these two clouds (i.e., reference and deformed point clouds) can be calculated using various methods, such as the M3C2 method (Seo et al., 2021). The M3C2 method has shown a great performance in estimating the deformation of point clouds due to its principles that calculates the distance between two local surfaces of the reference and deformed clouds (Lague et al., 2013).

In this research, the aim is to study the thermal impact on structures with different orientations using measurements for a case study of sheet piles. This is achieved by studying each part of the sheet piles with respect to its location and surface orientation. This is important to help designers to control the impact of thermal deformation, especially with the climate change that will increase the variation between thermal load between seasons, and hence the magnitude of seasonal deformations.

2 Measurements

Field measurements were taken for a sheet-pile retaining wall that was designed to resist the lateral stress from the soil and the hydro-static pressure from the canal. The flanges of the GU8N sheet piles were facing south, and a reinforced concrete capping beam was located on top of the sheet piles to strengthen the lateral resistance of the sheet piles and distribute the loads of the brick wall on top of the capping beam. Figure 1 shows the monitored part of the sheet piles (i.e., area of interest).

Figure 1. The monitored part of the sheet piles. The red box has dimensions of 3.5 m x 1 m.

The sheet piles were scanned using a TLS (Leica RTC360) in June and November between 2020 and 2022, with a total of five epochs starting from November 2020. The building is a new-build student accommodation, and it was in-service by the end of the summer of 2020. Table 1 presents the date and time of each scanning day as well as the air temperature at the time of scanning, as taken from Met-Office (nd). The monitoring was conducted from a scanning distance of 18 m, with a perpendicular scanning orientation with respect to the flanges of the sheet piles.

Table 1. Information for the scanning sessions

Epoch	Date	Time	Air temperature ($^{\circ}C$)
1	04/Nov/20	11:00	5.8
2	09/Jun/21	10:05	11.2
3	22/Nov/21	10:19	5.2
4	01/Jun/22	10:24	19.5
5	03/Nov/22	10:06	7.0

The TLS that was used in this case study, was tested under controlled experiments as presented in Algadhi et al. (2025). The results showed that the TLS had an accuracy of $1-2$ mm in detecting small geometric deformations, especially lateral displacements between $2-16$ mm.

3 Point cloud processing and deformation analysis

The scanning setup including the location of the TLS and the four targets as well as the monitored structure is presented in Figure 2. The local coordinate system was defined using the first scan on the 4^{th} of November 2020. The coordinate system on that day was rotated in the $x-y$ plane to align the $y-$axis with the lateral axis of the flanges of the sheet piles, and $x-$axis was parallel to the transverse axis of the sheet piles. The $z-$axis remained parallel to the longitudinal axis of the sheet piles (i.e., along their height). All the other scans were then transformed to this local coordinate system to allow for the deformation analysis.

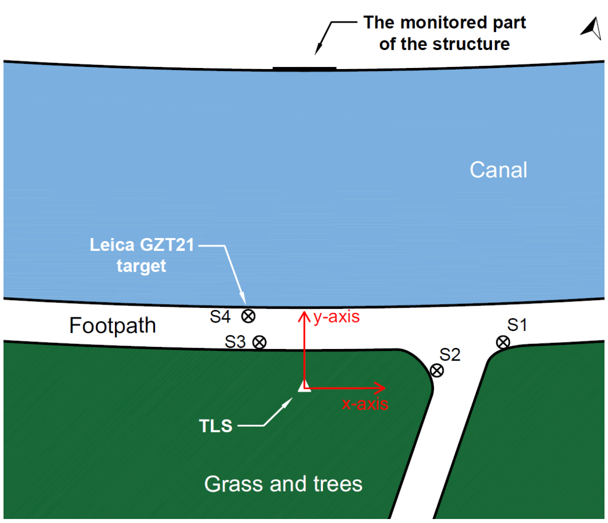

Figure 2. Plan view of the scanning field (not to scale). The sheet piles were 18 m away from the scanner, whereas the four targets S_1, S_2, S_3 and S_4 were 12 m, 10 m, 3 m and 6 m, respectively

Four static points were used on the side of the canal where the scanning was conducted. These targets were then used to register the point clouds that were taken at different epochs using the least squares adjustment method to solve for the seven unknown parameters (i.e., three translations, three rotations, and one scale parameter). The four static points provide twelve known equations, and the additional five known equations allowed the least squares adjustment method to iterate to find the statistical solution for the seven unknown parameters that will best fit the four static points in the point clouds to their coordinates in the local coordinate system.

A top and front views of the sheet piles in the final coordinate system is plotted in Figure 3 for the scan that was taken on the 4^{th} of November 2020. The normals of the sheet piles were calculated for each point, with a diameter of 0.02 m to estimate the normal vector for that local surface. The $x-$component of the normal vector separates the different parts of the sheet piles.

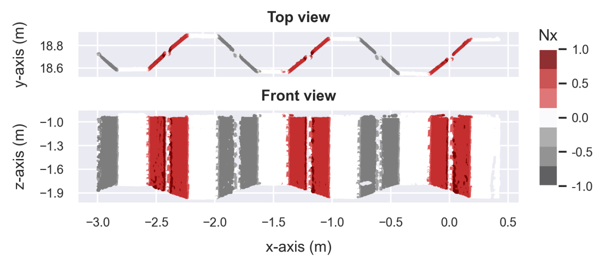

Figure 3. Top and front views of the sheet piles, showing the $x-$component of the normal vector

The sheet piles were segmented into different parts to allow for the deeper analysis of the individual parts of the sheet piles. The point clouds were segmented using the location and the normal vector of the points, as shown in Figure 4.

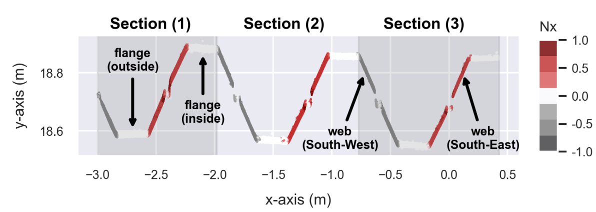

Figure 4. Top view of the sheet piles, showing the separated parts and sections of the sheet piles. Each section includes (i) inside flange, (ii) outside flange, (iii) South-West faced webs, and (iv) South-East faced webs. The sections are in order from left to right (i.e., West to East).

The deformation analysis was done using the M3C2 method, and by using the scan that was taken on the 4^{th} of November 2020 as the reference point cloud while the other scans were considered the deformed scans (i.e., at the latter epochs). The M3C2 distance was then calculated for each point in the reference point cloud by first estimating the normal direction for that point using the neighbouring points, with a diameter of 0.02 m. A cylinder was then project from the reference point cloud to the deformed cloud with a projection scale of $0.02\,m$. The maximum depth of this cylinder (i.e., the maximum expected deformation) was set to be $0.1\,m$.

In the case of sheet piles, the estimation of the normal direction from which the deformation is calculated is important since the sheet piles do not follow a particular orientation. Hence, the M3C2 method is the most suitable technique to estimate the deformation in the sheet piles.

4 Results and discussion

The deformation results show around $\pm 3-4\,mm$ of seasonal deformation in the sheet piles (Figure 5, caused mainly by the change in solar radiation. This deformation varied based on the surface orientation of each part of the sheet piles. The variation in deformation between the different parts of the sheet piles was detected at all epochs (i.e., in all months; June and November, and in all years; 2021 and 2022).

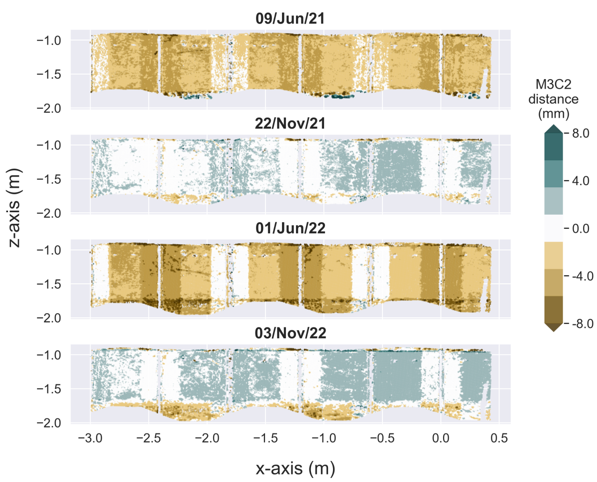

Figure 5. Front view of the sheet piles showing the deformation at each scanning day, compared to the scan in November 2020

After segmenting the sheet piles, as shown earlier in Figure 4, the deformation of each part of the sheet piles is presented in Figure 6. The results show similar performance for the inside and outside flanges in June and November of 2021 and 2022. This is because the surface orientation of these flanges were the same. In contrast, the webs had different performances as the orientation of their surfaces were different. The webs that were facing South-West had larger deformation, especially in June because their surface orientation was the most perpendicular to the sunlight. This was because the monitored structure was at a slight angle towards the West as shown earlier in Figure 2.

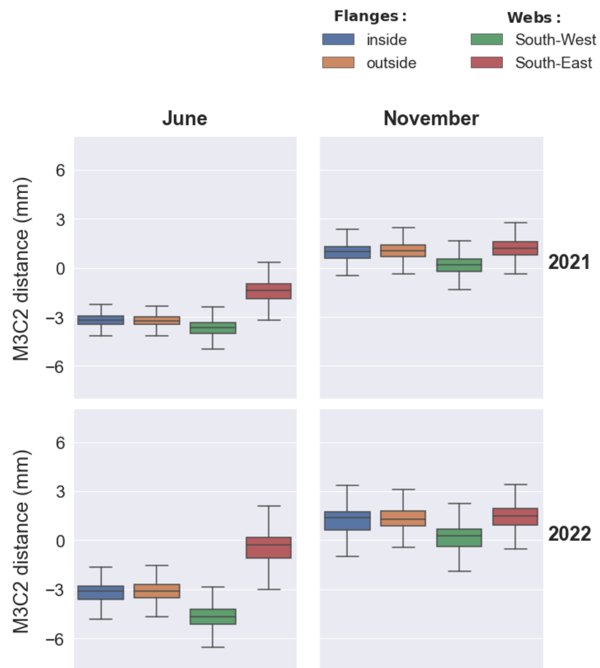

Figure 6. Deformation of each part of the sheet piles. The outliers were removed from the box plot to enhance clarity of the figure.

The webs that were facing South-East had the smallest seasonal deformation because they were the least affected by the sun because they were most of the time under the shadow. These webs had a performance similar to the flanges in November and had smaller deformation in June. The spread of the M3C2 distance measurements were similar for all the parts because all parts were built with the same material.

The deformation did also vary for each section (the sections are shown in Figure 4). Figure 7 shows the deformation of each section and in different months. There was a clear variation between the sections for all webs and flanges. As the structure curves (Figure 2), the normal vector for the flanges gets less aligned with the direction of the sunlight (i.e., South at noon time in the UK). Hence, the thermal deformation is less for the sections that are with an angle with respect to South. The normal vector of the nearly South-West oriented webs was the closest to the closest to the direction of the sunlight, and therefore had the largest deformation. The variation of deformation between June and November was the lowest for the South-East oriented webs because they were behind the shadow most of the time.

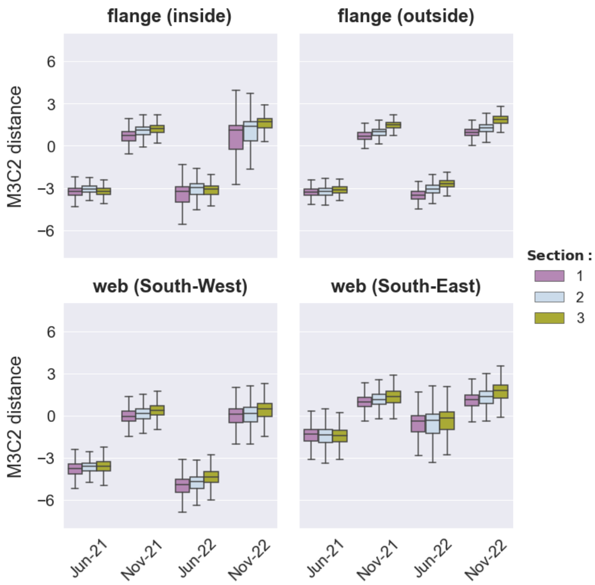

Figure 7. Deformation of each section of the sheet piles. The outliers were removed from the box plot to enhance clarity of the figure.

Solar radiation analysis has been conducted for the sheet piles in Autodesk Revit (Figure 8) given the location of the structure (Nottingham, UK) and its orientation with respect to north, as shown earlier in Figure 2. The analysis results shows the cumulative solar radiation on the various surfaces of the sheet piles for one sample day (01/June/2021) from the sunrise to the sunset. The areas which are in yellow were the most subjected to sunlight whereas the blue areas were the least.

The results from the solar radiation analysis confirms the deformation measurements from the laser scanner; showing that the south-west facing webs were the most subjected to solar radiation and hence had the largest thermal deformation (1.5 *mm* difference in comparison to the flanges), and the south-east facing webs were least subjected to sunlight and therefore, had the least thermal deformation. Figure 9 shows a clear pattern for the relationship between the solar radiation and the observed deformation in the sheet piles. The observed deformation increased in a banana-shaped curve as the solar radiation increased.

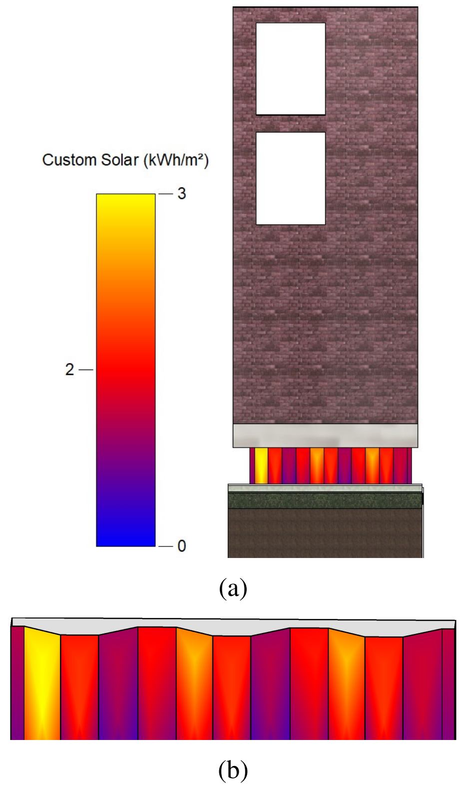

Figure 8. Solar radiation analysis for the sheet piles

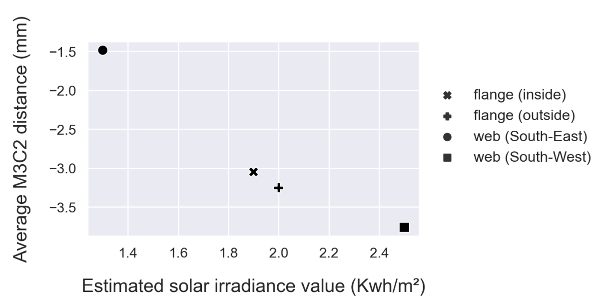

Figure 9. Scatter plot showing the relationship between the cumulative solar radiation and the calculated thermal deformation in June 2021 using the average M3C2 distance

5 Conclusion

A study was conducted for sheet-pile type of retaining wall because of its shape that has different surface orientations. The study was conducted for the lateral displacement caused by the seasonal variation of solar radiation. The field measurements were taken using a TLS and the processing was done for the point clouds of five epochs between November 2020 (just after completion of construction) and November 2022, with two scanning sessions each year (i.e., June and November). The sheet piles were segmented into different parts (i.e., webs and flanges) and different sections depending on the location.

The results showed a clear pattern for the deformation between June and November for all parts. The flanges, both inside and outside, had similar performance because they had the same orientation with respect to the sunlight. The webs, however, had different deformations. The South-West oriented webs had larger deformation than the other parts of the sheet pile because they were the most exposed part to the sunlight whereas the South-East webs had the lowest deformation as they were under the shadow most of the time. The deformation also varied for each section because the sheet piles were installed in a curve shape, and the section that was oriented towards the South had the largest deformation.

The results of this research is of great importance for designing the orientation of structures to limit their seasonal deformation. Further research should focus on monitoring various type of material and colour to investigate their impact on the seasonal deformation. Furthermore, the monitoring can be more detailed (i.e., with a higher measurement frequency) to investigate the thermal impact at different times of the year.

Acknowledgements

The authors extend their appreciation to the Deputyship for Research & Innovation, Ministry of Education in Saudi Arabia for funding this work.

References

Algadhi, A., Psimoulis, P., Grizi, A., and Neves, L. (2025). Experimental assessment of the performance of terrestrial laser scanners in monitoring the geometric deformations in retaining walls. *Journal of Civil Structural Health Monitoring*, pages 1–16.

Apriyono, A., Yuliana, and Kamchoom, V. (2022). Serviceability of cut slope and embankment under seasonal climate variations. *Acta Geophysica*, 71(2):983–995.

Breña, S. F., Bonczar, C. H., Civjan, S. A., DeJong, J. T., and Crovo, D. S. (2007). Evaluation of Seasonal and Yearly Behavior of an Integral Abutment Bridge. *Journal of Bridge Engineering*, 12(3):296–305.

Chwieduk, D. and Bogdanska, B. (2004). Some recommendations for inclinations and orientations of building elements under solar radiation in Polish conditions. *Renewable Energy*, 29(9):1569–1581.

Jafarkazemi, F. and Saadabadi, S. A. (2013). Optimum tilt angle and orientation of solar surfaces in Abu Dhabi, UAE. *Renewable Energy*, 56:44–49.

Kromanis, R. and Kripakaran, P. (2016). SHM of bridges: characterising thermal response and detecting anomaly events using a temperature-based measurement interpretation approach. *Journal of Civil Structural Health Monitoring*, 6(2):237–254.

Lague, D., Brodu, N., and Leroux, J. (2013). Accurate 3d comparison of complex topography with terrestrial laser scanner: Application to the rangitikei canyon (n-z). *ISPRS Journal of Photogrammetry and Remote Sensing*, 82:10–26.

Met-Office (n.d.). Watnall (Nottinghamshire) UK climate averages. Available from: <https://www.metoffice.gov.uk/research/climate/maps-and-data/uk-climate-averages/gcrje93b8> [Accessed 10/05/2024].

Portmann, R. W., Solomon, S., and Hegerl, G. C. (2009). Spatial and seasonal patterns in climate change, temperatures, and precipitation across the united states. *Proceedings of the National Academy of Sciences*, 106(18):7324–7329.

Seo, H., Zhao, Y., and Chen, C. (2021). Displacement Estimation Error in Laser Scanning Monitoring of Retaining Structures Considering Roughness. *Sensors*, 21(21):7370.

Westgate, R., Koo, K.-Y., and Brownjohn, J. (2015). Effect of Solar Radiation on Suspension Bridge Performance. *Journal of Bridge Engineering*, 20(5):04014077.